Steel and Composite Structures, *Vol. 19, No. 5 (2015) 1077-1094*
DOI: http://dx.doi.org/10.12989/scs.2015.19.5.1077

Slender RC columns strengthened with combined CFRP and steel jacket under axial load

Yi-yan Lu [a], Na Li [b], Shan Li [*1] and Tian-yan Ou [c]

School of Civil Engineering, Wuhan University, Wuhan City, Hubei Province, China

(*Received February 19, 2014, Revised June 20, 2014, Accepted April 15, 2015*)

Abstract. This paper presents an experimental study on the effectiveness of simultaneous application of carbon fiber-reinforced polymer (CFRP) and steel jacket in strengthening slender reinforced concrete (RC) column. The columns were 200 mm square cross section with lengths ranging from 1600 to 3000 mm. Ten columns were tested under axial load. The effects of the strengthening technique, slenderness ratio, cross-section area of steel angle and CFRP layer number were examined in terms of axial load-axial strain curve, CFRP strain, steel strip strain and steel angle strain. The experiments indicate that strengthening RC columns with combined CFRP and steel jacket is effective in enhancing the load capacity, ductility and energy dissipation capacity of RC column. Based on the existing models for RC columns strengthened with CFRP and with steel jacket, a design formula considering a slenderness reduction factor is proposed to predict the load capacity of the RC columns strengthened with combined CFRP and steel jacket. The predictions agree well with the experimental results.

Keywords: reinforced concrete column; strengthening; steel jacket; CFRP; axial load; load capacity

1. Introduction

Steel jacketing and FRP wrapping are used widely to strengthen the reinforced concrete (RC) columns. Steel jacketing is realized applying four corner steel angles to which discontinuous steel strips are welded. This technique can improve the load capacity, stiffness and ductility of RC columns and reduce the risk of buckling of longitudinal bars (Campione 2012a, Giménez *et al.* 2009, Cirtek 2001). However, the lateral confinement provided by the steel angles and strips is applied to the plane, effective only in a portion of the section's core, and further reduced in the volume of concrete between two strips (Montuori and Piluso 2009). Furthermore, outward buckling of the steel angles in the pitch of horizontal steel strips reduces its load capacity (Badalament 2010, Campione 2012b).

For the strengthening technique of FRP wrapping, FRP is wrapped around the RC columns to provide lateral confinement. This technique has proved to be effective in enhancing the ductility

*Corresponding author, Ph.D., E-mail: lsdlut@163.com
[a] Ph.D., Professor, E-mail: yylu901@163.com
[b] Ph.D. Student, E-mail: ln950228@163.com
[c] Ph.D. Student, E-mail: Outianyan@csepdi.com

Copyright © 2015 Techno-Press, Ltd.
http://www.techno-press.org/?journal=scs&subpage=8 ISSN: 1229-9367 (Print), 1598-6233 (Online)

and axial load capacity particularly for short columns (El-Hacha and Mashrik 2012, Campione *et al*. 2007, Ilki *et al*. 2008, Dai *et al*. 2011, Bai *et al*. 2014). However, the enhancement for square and rectangular columns is much lower than that for circular columns. This is attributed to the non-uniformity in confinement and the high stress concentration at the corners (Maaddawy *et al*. 2010, Harrie and Carey 2003). In slender RC column, the FRP confinement is less efficient than in short column, which is attributed to the second order effect (El-Hacha and Abdelrahman 2013, Gajdosova and Bilcik 2013).

The simultaneous use of FRP and steel jacket of strengthening RC columns may result in a more effective strengthening system than using single material, either FRP or steel jacket. In the strengthening system, the steel jacket provides axial resistance because of the coupled action of the confinement and the load carried by the steel angels, and also provides enhancements in flexural stiffness and tensile capacity, whereas the CFRP sheets provides confinement to the concrete along the whole height, relieving the confinement degeneration between two successive steel strips. The confinement provided by CFRP sheets restrains the concrete expansion in hoop direction and improves the deformability in axial direction, improving the dilation behavior. Experimental and theoretical studies carried out by Lu *et al*. (2003, 2006, 2005 and 2007) demonstrated the effectiveness of the combined CFRP and steel jacket strengthening system in enhancing RC columns under concentric load, eccentric load, shear load and cyclic load. Li *et al*. (2009) investigated the seismic behavior of corrosion-damaged reinforced concrete columns strengthened with combined CFRP and steel jacket. The results showed that strengthening corroded RC column with combined CFRP and steel jacket was more effective than strengthening only with steel jacket or CFRP sheets in improving the strength and ductility.

This study investigated the effects of the strengthening technique, the slenderness ratio, the cross-sectional area of steel angle and the CFRP layer number on the behavior of slender RC columns strengthened with combined CFRP and steel jacket under concentric compression load. Design formula for predicting the load capacity of RC columns strengthened with combined CFRP and steel jacket under axial load is presented.

2. Experimental program

2.1 Specimens details

The original RC columns were 200 mm square cross section ($b \times b$) with length (L) ranging from 1600 to 3000 mm. Four 16 mm diameter deformed bars were used as longitudinal reinforcement. Stirrups of 6 mm diameter bars were spaced at every 200 mm, which reduced to 50 mm at the ends of the RC columns. The details of the original RC columns are shown in Fig. 1.

2.2 Material properties

The steel type had a yield stress of 345 MPa for 16 mm diameter deformed bars and 245 MPa for 6 mm diameter bars and the concrete used in the columns had a 28-day cube compressive strength of 41 MPa. The material properties of CFRP for the nominal thickness, tensile stress, elastic modulus and elongation were 0.167 mm, 3500 MPa, 235 GPa and 2.1%, respectively. Steel angles L30 × 3 mm, L40 × 4 mm and L50 × 5 mm were used. Steel strips of 170 × 20 × 2 mm were welded to angles. The material properties of the steel angles and steel strip are shown in Table 1.

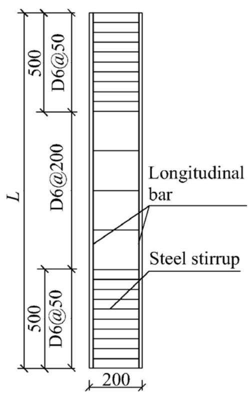

Fig. 1 Details of original columns (all dimensions in mm, *D* = diameter, *L* = length)

Table 1 Geometrical and mechanical properties of the steel angles and the steel strip

Element	Cross-section (mm)	Yield stress (MPa)	Ultimate stress (MPa)	Elongation (%)
Steel angel L30 × 3	50 × 50 × 5	288	432	20
Steel angel L40 × 4	40 × 40 × 4	288	425	24
Steel angel L50 × 5	30 × 30 × 3	316	426	28
Steel strip	170 × 20 × 2	355	460	23

Table 2 Details of the specimens

Specimen	*L* (mm)	*b* (mm)	*L*/*b*	Strengthening method
RC1	1600	200	8	Non-strengthened
RC2	1600	200	8	One layer of CFRP sheet
RC3	1600	200	8	Steel angel L40 × 4 and steel strip spacing 200 mm
RC4	1600	200	8	Steel angle L40 × 4, steel strip spacing 200 mm and one layer of CFRP sheet
RC5	2000	200	10	Steel angle L40 × 4, steel strip spacing 200 mm and one layer of CFRP sheet
RC6	2400	200	12	Steel angle L30 × 3, steel strip spacing 200 mm and one layer of CFRP sheet
RC7	2400	200	12	Steel angle L40 × 4, steel strip spacing 200 mm and one layer of CFRP sheet
RC8	2400	200	12	Steel angle L40 × 4, steel strip spacing 200 mm and two layers of CFRP sheets
RC9	2400	200	12	Steel angle L50 × 5, steel strip spacing 200 mm and one layer of CFRP sheet
RC10	3000	200	15	Steel angle L40 × 4, steel strip spacing 200 mm and one layer of CFRP sheet

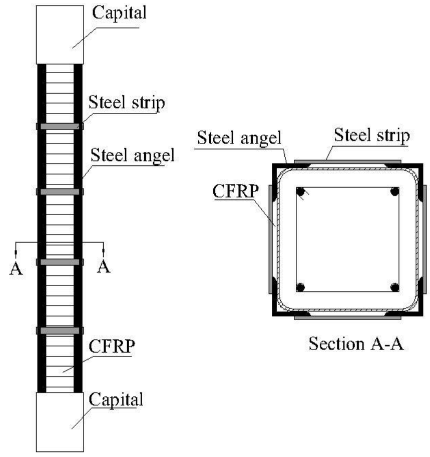

Fig. 2 RC column strengthened with combined CFRP and steel jacket

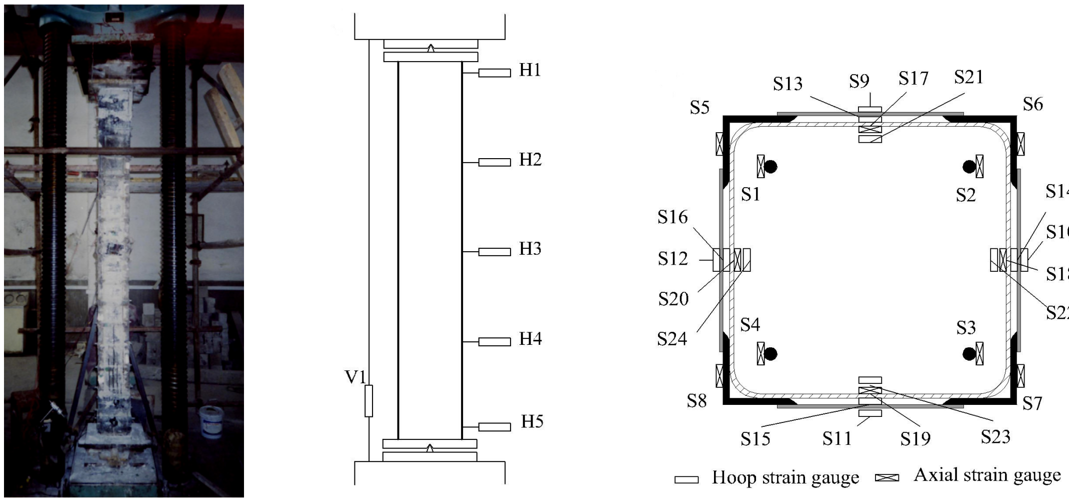

(a) Test set-up (b) Layout of LVDT (c) Arrangement of strain gauges

Fig. 3 Test set-up and arrangement of LVDTs and strain gauges

2.3 Strengthening procedure

Three strengthening techniques were used to strength the RC columns. The details of specimens are shown in Table 2. Prior to applying strengthening materials, the surface of RC columns was ground to obtain uniform surface, and the corners were rounded to a radius of 20 mm. CFRP sheets were wrapped along the whole column in transverse direction. Steel jacket was made up of four corners angles to which discontinuous horizontal steel strips were welded. Corner angles were epoxy-bonded to the concrete without gaps along the entire height. For the specimens strengthened with combined CFRP and steel jacket, the CFRP sheets were bonded in transverse direction firstly, and then four steel angels were fixed to the corners of the RC columns (Fig. 2).

2.4 Test set-up and instrumentation

Axial deformation of the specimens was measured by LVDT (V1) mounted between specimen ends. Lateral displacement of the specimens was measured using five horizontal LVDTs (H1-H5) at equally spaced locations along the column height (Fig. 3(b)). Strains of all materials at mid-height were monitored during loading. In each specimen, eight strain gauges were applied to the surface of concrete, four strain gauges were placed horizontally at each of the four faces and another four were placed vertically over horizontal strain gauges, and four strain gauges were used to measure the strains of longitudinal bars. The specimen strengthened with CFRP sheets had one strain gauge attached to the CFRP on each face, the specimen strengthened with steel jacket had four strain gauges attached to the steel angles and another four strain gauges attached to the steel strips. For the specimens strengthened with combined CFRP and steel jacket, each specimen had 24 strain gauges installed to measure strains (S1-S4, longitudinal bars, S5-S8, steel angles, S9-S12, steel strips, S13-S16, CFRP sheets, S17-S24, concrete), as shown in Fig. 3(c).

3. Failure modes

The failure of the non-strengthened specimen (RC1) was due to the concrete crushing. In the case of the specimen strengthened with CFRP (RC2), the failure occurred because of the fracture of CFRP beside one, or more of the corners, followed by the buckling of longitudinal bars. For the specimen strengthened with steel jacket (RC3), the failure occurred due to the concrete crushing. Along with concrete crushing, the steel angels on the most compressed side buckled outward.

As for the specimens strengthened with combined CFRP and steel jacket, the failure was due to the fracture of CFRP near the mid-height induced by the concrete crushing. The buckling of steel angles occurred after the ultimate load, with large lateral displacement (Fig. 4). The length of CFRP fractured along the column height varied depending on slenderness ratio and cross-sectional area of steel angels. For specimens RC4, RC5, RC7 and RC10, the length decreased from 400 mm to 150 mm with the slenderness ratio increasing from 8 to 15. For specimens RC6, RC7 and RC9, the length increased with the increasing of cross-sectional area of steel angels.

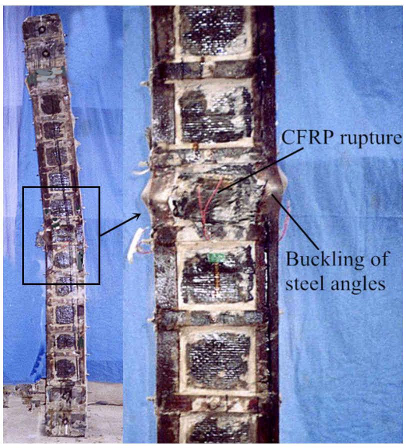

Fig. 4 Typical failure mode of the specimens strengthened with combined CFRP and steel jacket

4. Experimental results and discussions

The ultimate load and ultimate axial strain of the specimens are shown in Table 3. The axial strain is represented by the average axial strain recorded by four strain gauges mounted to concrete surface. Ductility and energy dissipation capacity are used as parameters for the evaluation of slender columns. The ductility is defined as the ratio of the axial strain at ultimate load and the yield strain, which is taken as the axial strain ε_{75} divided by 0.75, where ε_{75} is the axial strain prior to failure, corresponding to 75% of the ultimate load. The parameter of the energy dissipation capacity composes of the unit energy dissipation capacity and the column energy dissipation capacity. The unit energy dissipation capacity is the area under the axial load-axial strain curve up to the ultimate load. The column energy dissipation capacity is given by the product of unit energy dissipation capacity for the height of column. The ductility and energy dissipation capacity of the specimens are also shown in Table 3.

Table 3 Test results of the specimens

Specimen	Ultimate load (kN)	Ultimate axial strain ($\mu\varepsilon$)	Ductility	Unit energy dissipation capacity (kN·mm/mm)	Column energy dissipation capacity (kN·mm)
RC1	1420	1670	1.30	1.40	2240
RC2	1550	2275	1.36	2.28	3648
RC3	1880	2350	1.52	2.96	4736
RC4	2130	2965	1.71	4.34	6944
RC5	2100	2625	1.57	3.67	7340
RC6	1880	1908	1.30	2.16	5184
RC7	2080	2156	1.37	2.87	6888
RC8	2100	2791	1.87	4.28	10272
RC9	2350	2063	1.47	3.22	7728
RC10	1850	1953	1.43	2.39	7170

Table 4 Strains of CFRP, steel strip and steel angle for the specimens

Specimen	Average ultimate strain of CFRP ($\mu\varepsilon$)	Average ultimate strain of steel strip ($\mu\varepsilon$)	Average ultimate strain of steel angle ($\mu\varepsilon$)
RC1	–	–	–
RC2	732	–	–
RC3	–	433	1997
RC4	2629	1063	2002
RC5	1482	863	1816
RC6	794	184	1478
RC7	1137	737	1850
RC8	2145	1198	1541
RC9	1406	963	1930
RC10	949	343	1137

The confinement to concrete can be assessed by evaluate the ultimate lateral strains developed in the CFRP sheets and steel strips. The load carried by steel angles was expressed by the longitudinal strain of steel angle. The average strains of CFRP, steel strips and steel angels, calculated from the strains recorded by the corresponding strain gauges, are shown in Table 4.

4.1 Effect of different strengthening techniques

In this study, three different strengthening techniques were investigated. To evaluate the effectiveness of different strengthening techniques, specimens RC1, RC2, RC3 and RC4 were compared in terms of axial load-axial strain curve, as shown in Fig. 5. The enhanced behavior of the strengthened RC columns compared with the non-strengthened RC columns was observed. For specimens RC2, RC3 and RC4, comparing with specimen RC1, the enhancement in the ultimate load was 9.1%, 32.4% and 50.0%, respectively, and that in the ultimate axial strain was 36.2%, 40.7% and 77.5%, respectively.

The increased ultimate load and the failure axial strain of the composite columns indicated enhancement in the ductility and energy dissipation capacity. The ductility and energy dissipation capacity are shown in Table 3. Comparing with specimen RC1, specimens RC2, RC3 and RC4 had an increase in the ductility by 4.6%, 16.9% and 31.5%, respectively. The energy capacity increased by 62.8%, 111.4% and 210.0%, respectively, for specimens RC2, RC3 and RC4, when compared with specimen RC1.

The average ultimate strains of the CFRP, the steel strip and the steel angel are shown in Table 4. As can be inferred from Table 4, the simultaneous use of CFRP and steel jacket was beneficial to the confinement efficiency of both CFRP and steel jacket, whereas had no obvious influence on the average strain of steel angel.

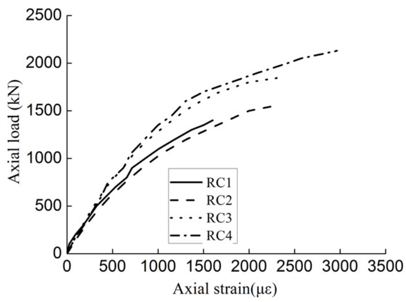

Fig. 5 Axial load-axial strain curves for specimens RC1, RC2, RC3 and RC4

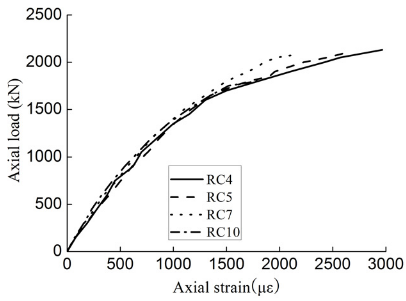

Fig. 6 Axial load-axial strain curves for specimens RC4, RC5, RC7 and RC10

4.2 Effect of slenderness ratio

The effect of slenderness ratio on the behavior of specimens strengthened with combined CFRP and steel jacket can be evaluated by comparing the test results of specimens RC4, RC5, RC7 and RC10. The results are discussed in terms of axial load-axial strain curve, ultimate CFRP strain, ultimate steel strip strain and ultimate steel angle strain.

Fig. 6 shows the axial load-axial strain curves for specimens RC4, RC5, RC7 and RC10. The ultimate load and ultimate axial strains reduced with the increasing of the slenderness ratio. For specimens RC5, RC7 and RC10, the ultimate load reduced by 1.4%, 2.4% and 13.1%, respectively, and the ultimate axial strain reduced by 11.4%, 25.6% and 34.1%, respectively, in comparing with specimen RC4. It can be seen from Table 3 that increasing the slenderness ratio reduced the ductility and unit energy dissipation capacity of the specimens. In comparison with the unit energy dissipation capacity of the specimens with a slenderness ratio of 8, increasing the slenderness ratio decreased the unit energy dissipation capacity by 15.4%, 33.9% and 44.9% for the specimens with slenderness ratio of 10, 12 and 15, respectively. However, the variation in the column energy dissipation capacity seems not depend on the slenderness ratio. Thus, increasing the height resulted in reduced performance of the columns strengthened with combined CFRP and steel jacket.

The reduced performance of the specimens with the increasing of slenderness ratio was related to the low and non-uniform confinement pressure. The non-uniform confinement pressure can be verified by plotting the strains versus different sides of columns. Figs. 7(a) and (b) demonstrate the distribution of ultimate lateral strains over the perimeter of the CFRP sheets and the steel strips, respectively. Number “1” denotes the most compressed side, number “3” denotes the least compressed side and number “2” denotes the other two sides. The lateral strains of CFRP and steel strip at different sides fluctuated widely. The ratio of minimum and maximum strain for CFRP ranged between 0.13 and 0.35, while that for steel strips between 0.20 and 0.41, indicating non-uniform confinement to concrete.

The confinement pressure is also can be expressed by the average ultimate stains of CFRP and steel strip (see Table 4). The ultimate strains of CFRP were significantly less than the CFRP fractured strain obtained from tensile tests on the CFRP coupons, and ultimate strains of the steel strips did not reach the yield stain. The average ultimate strains of CFRP and steel strip reduced with the increasing of the slenderness ratio. When the slenderness ratio increased from 8 to 15,

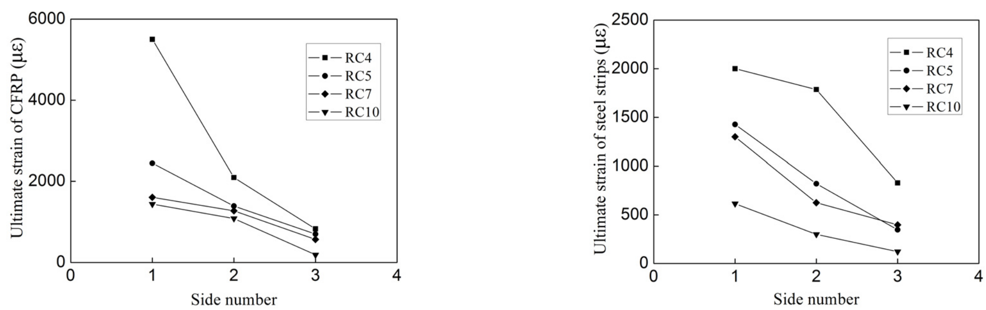

(a) Ultimate lateral strain of the CFRP (b) Ultimate lateral strain of the steel strips

Fig. 7 Distribution of ultimate strain of materials for specimens RC4, RC5, RC7 and RC10 the decrease in the average ultimate strain of CFRP was 63.9%, and that in the average ultimate strain of steel strip was 78.6%. Thus, the increasing in the slenderness ratio reduced the confinement effectiveness of the CFRP sheets and steel strips.

In addition, increasing the slenderness ratio resulted in decreasing the strain of steel angle, which was attributed to the reduction of ultimate load. The average strains of steel angels are shown in Table 4. Similar ultimate strains of steel angel were recorded in specimens RC4, RC5 and RC7 and were considerably reduced in specimen RC10, which is assumed to be another cause for the significant decrease of load capacity.

4.3 Effect of cross-sectional area of steel angle

To determine the effect of the cross-sectional area of steel angle on the strengthening of the specimens strengthened with combined CFRP and steel jacket, specimens RC6, RC7 and RC9 were studied in terms of axial load-axial strain curve, ultimate CFRP strain, ultimate steel strip strain and ultimate steel angle strain.

Fig. 8 presents the axial load-axial strain for specimens RC6, RC7 and RC9. This figure shows that with the increasing of the cross-sectional area of steel angel, the ultimate load increased. The ultimate loads and ultimate axial strains are shown in Table 3. In comparison with the ultimate load of specimen RC6 with 30 × 30 × 3 mm steel angel, using the steel angle with cross section of 40 × 40 × 4 mm and 50 × 50 × 5 mm obtained an axial load enhancement by 10.6% and 25.0%, respectively. The ductility and energy dissipation capacity of the specimens are shown in Table 4.

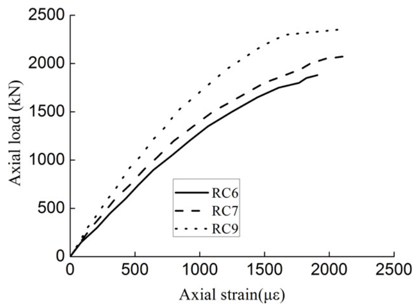

Fig. 8 Axial load-axial strain curves for specimens RC6, RC7 and RC9

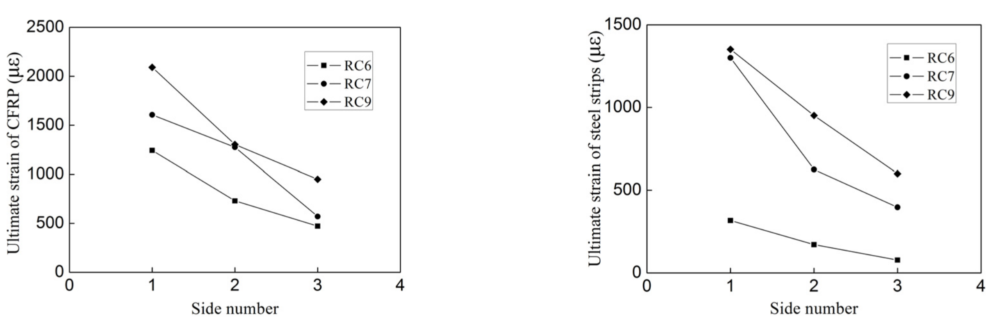

(a) Ultimate lateral strain of the CFRP (b) Ultimate lateral strain of the steel strips

Fig. 9 Distribution of ultimate strain of materials for specimens RC6, RC7 and RC9

For specimens RC7 and RC9, when compared with specimen RC6, the enhancement in the ductility was 5.4% and 13.1%, and that in the energy dissipation capacity 32.9% and 49.1%, respectively. Thus, increasing cross-sectional area of steel angle improved the performance of RC columns strengthened with combined CFRP and steel jacket.

The improved performance of the specimens with the increasing of cross-sectional area of steel angel was partially attributed to the enhancement confinement and the increasing load carried by steel angles. Fig. 9(a) illustrates the distribution of ultimate strains over the perimeter of the CFRP. The strain of CFRP on each side increased with the increasing of cross-sectional area of steel angels. The ratio of the minimum and maximum strain was 0.38, 0.35 and 0.45 for specimens RC6, RC7 and RC9, respectively. The average strains of CFRP for specimens RC6, RC7 and RC9 are shown in Table 4. The increase of average CFRP strains for specimens RC7 and RC9 was 43.2% and 77.1%, respectively, when compared with specimen RC 6.

Fig. 9(b) shows the distribution of ultimate strains over the perimeter of the steel strips. The strains of steel strips for specimens RC7 and RC9 were much larger than that of specimen RC6. The variation of steel strip strain at different sides decreased with the increasing of steel angel area (0.25 for specimen RC6, 0.31 for specimen RC7 and 0.44 for specimen RC9). The average strains of steel strips for specimens RC6, RC7 and RC9 are shown in Table 4. The strain of steel strips increased by 300.5% and 423.4% for specimens RC7 and RC9 in comparing with specimen RC6.

4.4 Effect of CFRP layers

The effect of CFRP layer number on the behavior of RC specimens strengthened with combined CFRP and steel jacket was determined by comparing specimens RC7 with specimen RC8 in terms of axial load-axial strain curve, ultimate CFRP strain, ultimate steel strip strain and ultimate steel angle strain. Fig. 10 shows the axial load-axial strain curves for specimens RC7 and RC8. Increasing the CFRP layer number led to no obvious enhancement in ultimate load, but a notable increase in axial strain. For the specimen with two layers of CFRP, the axial load increased rather slowly, but the axial load increased greatly when the axial load closed to the ultimate load. The ultimate axial strain increased by 29.4% with increased CFRP layer number (see Table 3). The increasing axial strain indicates significant improvement in ductility and energy dissipation capacity, as shown in Table 4. When the CFRP layer number increased, the increase in the ductility and energy dissipation capacity was 36.5% and 49.1%, respectively. Thus, increasing the CFRP layer number improves the performance of RC columns strengthened with combined CFRP and steel jacket.

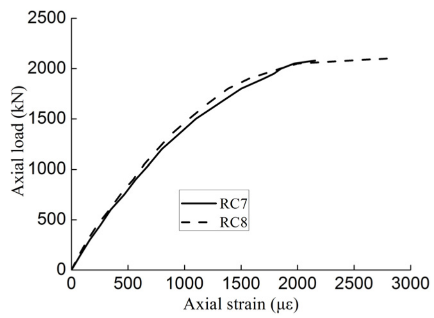

Fig. 10 Axial load-axial strain curves for specimens RC7 and RC8

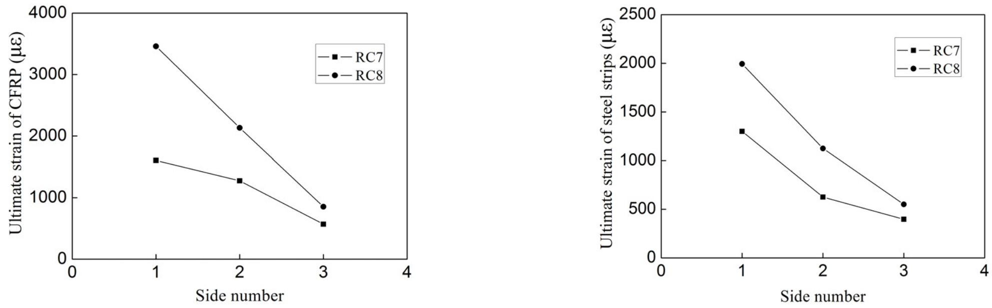

(a) Ultimate lateral strain of the CFRP (b) Ultimate lateral strain of the steel strips

Fig. 11 Distribution of ultimate strain of materials for specimens RC7 and RC8

When the CFRP layer number increased, the variation of the CFRP and steel strips strain at different sides reduced, as shown in Fig. 11. The ratio of minimum and maximum strain of CFRP reduced from 0.35 to 0.25 and that of steel strip from 0.31 to 0.28. The average ultimate strains of CFRP, steel strip and steel angel are shown in Table 4. Increasing the CFRP layer number increased the average ultimate strains of CFRP and steel strip by 88.6% and 62.5%, respectively. However, increasing of CFRP layer reduced the average ultimate strain of steel angels. Thus, increasing the CFRP layer number can increase the confinement effectiveness of CFRP and steel strips to concrete, but reduced the strength contribution of steel angles.

5. Prediction of load capacity

5.1 Section load capacity

For the RC column strengthened with combined CFRP and steel jacket, the section load capacity N can be calculated by considering the strength contributions of the concrete, the steel angles and longitudinal bars and expressed as follows

$$N = N_c + N_a + N_s \tag{1}$$

where N_c is the contribution of concrete, N_a is the contribution of steel angles, and N_s is the contribution of longitudinal steel bars.

5.1.1 Strength contribution of concrete

The effective confinement pressure f_l' on the concrete core in the columns strengthened with combined CFRP and steel jacket is expressed by

$$f_l' = f_{lf}' + f_{ls}' = \frac{k_{ef} \cdot \rho_{fv} \cdot E_f \cdot \varepsilon_{fe}}{2} + \frac{k_{es} \cdot \rho_{sv} \cdot f_{ys}}{2} \tag{2}$$

where f_{lf}' and f_{ls}' is the effective confinement pressures provided by CFRP and steel strip, respectively, k_{ef} is the confinement effectiveness coefficient for FRP, ρ_{fv} is the transverse reinforcement volumetric ratio for FRP, E_f is the modulus of elasticity of the composite, ε_{fe} is the

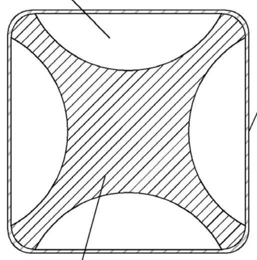

Fig. 12 Effectively confined region of square column due to arching action

lateral strain in CFRP at the point of rupture and equal to 0.005, k_{es} is the confinement effectiveness coefficient for steel strips, ρ_{sv} is the transverse reinforcement ratio for steel strips, and f_{ys} is the yielding stress of strip.

According to ACI 440.2R-02 (2002), the confinement effectiveness coefficient for FRP k_{ef} is

$$k_{ef} = \frac{A_e}{A_{cor}} = 1 - \frac{2(b-2r)^2}{3A_{cor}(1-\rho_s)} \tag{3}$$

where A_e and A_{cor} are the area of effectively confined concrete and the area of concrete after corner chamfering and calculated by $b^2-(4-\pi)\,r^2$, respectively, as shown in Fig. 12, r is the corner radius, and ρ_s is the reinforcement ratio of the longitudinal bars with respect to the original section area.

The transverse reinforcement volumetric ratio for FRP ρ_{fv} is defined as

$$\rho_{fv} = \frac{4n_f t_f b}{A_{cor}} \tag{4}$$

where n_f is the CFRP layer number and t_f is the thickness of single CFRP layer.

For the concrete strength enhancement due to the steel jacket, the lateral confinement pressure is effective only in a portion of the concrete core, and further reduced along the height (Fig. 13). Taking into account the confinement reduction in both cross section and height, Montuori and Piluso (2009) proposed a model for the confinement effectiveness coefficient k_{es} (see Eq. (5)).

$$k_{es} = \left[1 - \frac{2}{3}\cdot\frac{(b-2L_1)^2}{b^2}\right]\cdot\left(1-\frac{s-s_2}{2b}\right)^2 \tag{5}$$

where L_1 is the side length of steel angles, s is the center spacing between two successive steel strips, and s_2 is the width of steel strips.

The transverse reinforcement volumetric ratio for steel strips ρ_{sv} is expressed by

$$\rho_{sv} = \frac{4t_2 s_2}{bs} \tag{6}$$

where t_2 is the thickness of the steel strips.

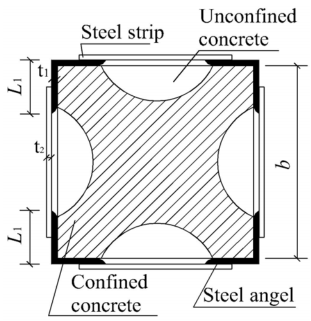

(a) In the plane of steel strips

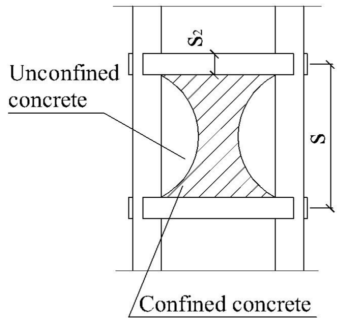

(b) Along the height between two successive strips

Fig. 13 Effectively confined region of column due to steel strips and angels (Montuori and Piluso 2009)

The strength model given by EC8 (2003) is used to calculate the confined compressive strength f'_{cc}, as shown in Eq. (7).

$$f'_{cc} = f'_c\left[1 + 3.7\left(\frac{f'_l}{f'_c}\right)^{0.87}\right] \tag{7}$$

where f'_c is the unconfined cylinder concrete compressive strength.

The expression of N_c is

$$N_c = f'_c b^2\left[1 + 2.02\left(\frac{k_{ef}\cdot\rho_{fv}\cdot E_f\cdot\varepsilon_{fe} + k_{es}\cdot\rho_{sv}\cdot f_{ys}}{f'_c}\right)^{0.87}\right] \tag{8}$$

Introducing into Eq. (8) the mechanical ratio of steel strips ω_s defined as

$$\omega_s = \rho_{sv}\cdot\frac{f_{ys}}{f'_c} \tag{9}$$

and the mechanical ratio of FRP ω_f defined as

$$\omega_f = \rho_{fv}\cdot\frac{f_{fu}}{f'_c} \tag{10}$$

in which f_{fu} is the tensile strength of FRP determined from coupon tests, results in

$$N_c = f'_c b^2\left[1 + 2.02(\omega_f\cdot k_{ef}\cdot\eta + \omega_s\cdot k_{es})^{0.87}\right] \tag{11}$$

where η is the strain efficiency for FRP and determined by $E_f\varepsilon_{fe}/f_f$.

5.1.2 Strength contribution of steel angle

For the contribution of steel angles, it has to be considered that the angles are subjected to the dual effects of axial force and bending moment. The bending moment is the consequence of the

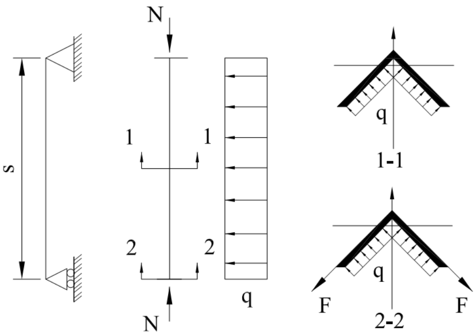

Fig. 14 Simplified model for steel angle (Badalamenti *et al*. 2010)

concrete expansion. The axial force is a result of the shortening of the column in the case of angles directly loaded. Badalamenti *et al*. (2010) proposed a simplified model to analyze the axial force in steel angels (Fig. 14). It consists of a fixed beam at the supports (strips) loaded in flexure along the symmetry plane with the resultant confining pressures $(q = \sqrt{2} f'_{ls} L_1)$ and also by axial loads.

According to Badalamenti *et al*. (2010), the maximum axial force available in single directly load angel N_a^* is given as

$$N_a^* = \sqrt{4 f_{ya} t_1 \left(f_{ya} t_1 L_1^2 - 4 M_a^* \right)} \tag{12}$$

in which f_{ya} is the yield strength of steel angels, t_1 is the thickness of steel strips, and the bending moment in single steel angles M_a^* is given as

$$M_a^* = \frac{q(s - s_2)^2}{12} \tag{13}$$

in which f_{ya} is the yield strength of steel angels, t_1 is the thickness of steel strips, and the bending moment in single steel angles M_a^* is given as

$$N_a = 8 f_{ya} t_1 L_1 \cdot \sqrt{1 - \frac{\sqrt{2}}{6} \cdot \frac{f_{ys} \rho_{sv} k_{es} (s - s_2)^2}{f_{ya} t_1 L_1}} \tag{14}$$

Introducing into Eq. (14) the mechanical ratio of steel strips ω_s and the mechanical ratio of steel angles ω_a defined as

$$\omega_a = \rho_a \cdot \frac{f_{ya}}{f'_c} \tag{15}$$

in which ρ_a is the reinforcement ratio of the steel angels with respect to the original section area, and defined as $8L_1 t_1 / b^2$, results in

$$N_a = 8 f_{ya} t_1 L_1 \cdot \sqrt{1 - 1.88 \cdot \frac{\omega_s}{\omega_a} \cdot \left(\frac{s - s_2}{b} \right)^2 \cdot k_{es}} \tag{16}$$

5.1.3 Strength contribution of longitudinal bar

In the composite strengthening system, the contribution of longitudinal bars is calculated, assuming an elastic-plastic behavior without buckling effects. This assumption is justified because the presence of the confinement provided by the steel jacket and CFRP reduces the risk of buckling. The contribution of longitudinal bars can be expressed by

$$N_s = f_{yl} A_s \tag{17}$$

where f_{yl} is the yield strength of longitudinal bar, and A_s is the total cross-sectional area of the longitudinal bars.

Substituting Eqs. (11), (16) and (17) into Eq. (1) results in the load capacity of the RC columns strengthened with combined CFRP and steel jacket

$$N_u = f_c' b^2 \left[1 + 2.02\left(\omega_f \cdot k_{ef} \cdot \eta + \omega_s \cdot k_{es}\right)^{0.87}\right] + 8 f_{ya} t_1 L_1 \cdot \sqrt{1 - 1.88 \cdot \frac{\omega_s}{\omega_a} \cdot \left(\frac{s - s_2}{b}\right)^2 \cdot k_{es}} + f_{yl} A_s \tag{18}$$

In order to evaluate the accuracy of Eq. (18) in predicting the section capacity of RC columns strengthened with combined CFRP and steel jacket, a comparison between the experimental results and the calculated results obtained with Eq. (18) is made. The data given in Lu *et al*. (2003) refer to six specimens with dimensions of 150 × 150 × 600 mm. Two of them were reinforced concrete columns with four longitudinal bars 12 mm in diameter with stirrups 6 mm in diameter and others were plain concrete columns. The yield strength of longitudinal bar was 310 MPa. The columns were strengthened with combined CFRP and steel jacket. The steel jacket composed of 30 × 30 × 3 mm steel angels at four corners and 120 × 20 × 2 mm rectangular steel battens welded to angles at pitch 150 mm. The yield strength for steel angle and steel batten were 275 and 320 MPa, respectively. The material properties of CFRP sheets used for the nominal thickness, tensile stress and elastic modulus were 0.167 mm, 5000 MPa and 235 GPa, respectively. The concrete used had a cubic strength of 34.7 MPa. Based on the comparison, the mean value and deviation of the ratio of experimental and calculated results are 1.08 and 0.077, respectively. Therefore, Eq. (18) can accurately predict the section load capacity of RC columns strengthened with combined CFRP and steel jacket.

5.2 Member load capacity

To calculate the load capacity of column members, the slenderness effect should be taken into consideration by introducing a slenderness reduction factor χ. The value of χ is determined from the buckling curve. According to EC3 (1993), it can be expressed as follows

$$\chi = \frac{1}{\phi + \sqrt{\phi^2 - \bar{\lambda}^2}} \tag{19}$$

in which

$$\phi = 0.5\left(1 + \alpha\left(\bar{\lambda} - 0.2\right) + \bar{\lambda}^2\right) \tag{20}$$

where α is an imperfection factor and equal to 0.21 for RC columns strengthened with combined CFRP and steel jacket, and $\bar{\lambda}$ is the relative slenderness ratio.

Table 5 Comparisons between the experimental and calculated results

Specimens	$\bar{\lambda}$	χ	N_e (kN)	N_p (kN)	N_e / N_p
RC4	0.37	0.96	2130	2118	1.00
RC5	0.46	0.93	2100	2063	1.02
RC6	0.54	0.91	1880	1882	1.00
RC7	0.56	0.90	2080	1997	1.04
RC8	0.56	0.90	2100	2186	0.96
RC9	0.58	0.89	2350	2162	1.09
RC10	0.70	0.85	1850	1872	0.99

For the columns strengthened with combined CFRP and steel jacket, $\bar{\lambda}$ is determined by

$$\bar{\lambda} = \sqrt{\frac{f'_c A_c + f_{ya} A_a + f_{yl} A_s}{\dfrac{\pi^2 (EI)_{eff}}{L^2}}} \tag{21}$$

where A_a is the cross-sectional area of steel angels and equal to $8L_1t_1$, and $(EI)_{eff}$ is the effective flexural stiffness. According to EC4 (2003), it can be determined as

$$(EI)_{eff} = E_s I_s + 0.6 E_c I_c + E_a I_a \tag{22}$$

where I_c, I_s and I_a are the second moments of area of the concrete section, the longitudinal bars and the steel angels for the bending plane being considered, respectively, and E_c, E_s and E_a are the modulus of elasticity of the concrete section, the longitudinal bars and the steel angels, respectively.

When the RC column strengthened with combined CFRP and steel jacket is referred to an equivalent steel column, $\bar{\lambda}$ can be given by

$$\bar{\lambda} = \frac{L}{r_0} \cdot \frac{1}{\pi \cdot \sqrt{\dfrac{E_a}{f_{ya}}}} = \frac{L}{\sqrt{\dfrac{E_s I_s / E_a + 0.6 E_c I_c / E_a + I_a}{A_s f_{yl} / f_{ya} + A_c f'_c / f_{ya} + A_a}}} \cdot \frac{1}{\pi \cdot \sqrt{\dfrac{E_a}{f_{ya}}}} \tag{23}$$

where r_0 is the equivalent radius of gyration about the relevant axis.

5.3 Comparison of experimental and calculated results

Table 5 shows the comparisons between the experimental results (N_e) and predicted results (N_p). The calculated results agree well with the experimental results. The mean value and the deviation of the ratio of experimental results and predicted results are 1.014 and 0.037.

6. Conclusions

- Strengthening technique of combined CFRP and steel jacket is effective in improving the ultimate load and ultimate axial strain of slender RC columns, and results in better ductility and energy dissipation capacity.

- In slender RC columns strengthened with combined CFRP and steel jacket, the confinement of CFRP sheets and steel strips uniformly distributes along the perimeter of column. The ratio of minimum and maximum strain for CFRP ranged between 0.13 and 0.45, while that for steel strips varied from 0.20 to 0.44.
- Increasing the slenderness ratio of RC columns strengthened with combined CFRP and steel jacket reduces confinement of CFRP and steel jacket to the concrete and the axial load carried by steel angels, resulting in a decrease in the ultimate load, ultimate axial strain, ductility and unit energy dissipation capacity.
- The use of steel angles with larger cross-section area has a beneficial effect on the ultimate load, ductility and energy dissipation capacity and leads to higher confinement of CFRP and steel jacket, and higher strength of steel angles.
- Increasing CFRP layers number leads to notable improvement in ultimate axial strain, ductility and energy dissipation capacity attributable to the higher confinement of CFRP and steel jacket, but slight increase in ultimate load.
- Design equations are proposed for predicting the load capacity of RC columns strengthened with combined CFRP and steel jacket. The predictions agree well with the experimental results.

Acknowledgments

The funding for this investigation was provided by the Young Scientist Project of the Natural Science Foundation of China (51108355), the Natural Science Foundation of Hubei Province, China (No. 2011CDB269), and the Fundamental Research Funds for the Central Universities, China (No. 2014210020201). The authors greatly appreciate their financial support.

References

ACI 440.2R-02 (2002), Guide for the design and construction of externally bonded FRP systems for strengthening concrete structures, Farmington Hills, MI, USA.

Badalament, V., Campione, G. and Mangiavillano, M.L. (2010), “Simplified model for compressive behavior of concrete columns strengthened by steel angles and strips”, *J. Eng. Mech.*, **136**(2), 230-238.

Bai, Y.L., Dai, J.G. and Teng, J.G. (2014), “Cyclic compressive behavior of concrete confined with large rupture strain FRP composites”, *J. Compos. Constr.*, **18**(1), 04013025.
DOI: 10.1061/(ASCE)CC.1943-5614.0000386

Campione, G. (2012a), “Load carrying capacity of RC compressed columns strengthened with steel angles and strips”, *Eng. Struct.*, **40**, 457-465.

Campione, G. (2012b), “Strength and ductility of R.C. columns strengthened with steel angles and battens”, *Constr. Build. Mater.*, **35**, 800-807.

Campione, G., Colajanni, P. and La, M.L. (2007), “Ductility of reinforced concrete members externally wrapped with fiber-reinforced polymer sheets”, *J. Compos. Constr.*, **11**(3), 279-290.

Cirtek, L. (2001), “RC columns strengthened with bandage - experimental programme and design recommendations”, *Constr. Build. Mater.*, **15**(8), 341-349.

Dai, J.G., Bai, Y.L. and Teng, J.G. (2011), “Behavior and Modeling of Concrete Confined with FRP Composites of Large Deformability”, *J. Compos. Constr.*, **15**(6), 963-973.

El-Hacha, R. and Mashrik, M.A. (2012), “Effect of SFRP confinement on circular and square concrete

columns" *Eng. Struct.*, **36**, 379-393.
El-Hacha, R. and Abdelrahman, K. (2013), "Slenderness effect of circular concrete specimens confined with SFRP sheets", *Compos. Part B- Eng.*, **44**(1), 152-166.
Eurocode 3 (1993), Design of steel structures. Part 1-1: General rules and rules for buildings, Brussels, Belgium.
Eurocode 4 (2004), Design of composite steel and concrete structures. Part 1-1: General rules and rules for buildings, Brussels, Belgium.
Eurocode 8 (2003), Design of structures for earthquake resistance. Part 3: Strengthening and repair of buildings, Brussels, Belgium.
Gajdosova, K. and Bilcik, J. (2013), "Full-Scale Testing of CFRP-Strengthened Slender Reinforced Concrete Columns", *J. Compos. Constr.*, **17**(2), 239-248.
Giménez, E., Adam, J.M., Ivorra, S. and Calderón, P.A. (2009), "Influence of strips configuration on the behaviour of axially loaded RC columns strengthened by steel angles and strips", *Mater. Design*, **30**(10), 4103-4111.
Harrie, K.A. and Carey, S.A. (2003), "Shape and "gap" effects on the behavior of variably confined concrete", *Cement Concrete Res.*, **33**(6), 881-890.
Ilki, A., Peker, O. and Karamuk, E. (2008), "FRP retrofit of low and medium strength circular and rectangular reinforced concrete columns", *J. Mater. Civil Eng.*, **20**(2), 169-188.
Li, J.B., Gong, J.X. and Wang, L.C. (2009), "Seismic behavior of corrosion-damaged reinforced concrete columns strengthened using combined carbon fiber-reinforced polymer and steel jacket", *Constr. Build. Mater.*, **23**(7), 2653-2663.
Lu, Y.Y., Shi, J.Y. and Zhao, G.F. (2003), "Experimental research on concrete columns strengthened with the combination of CFRP and angle steel", *J. Build. Struct.*, **24**(5), 18-23.
Lu, Y.Y., Chen, S.X. and Zhao, G.F. (2005), "An experimental study on the seismic behavior of reinforced concrete columns strengthened with bonded steel hoops and carbon fiber reinforced polymer sheet", *China Civ. Eng. J.*, **38**(8), 10-17.
Lu, Y.Y., Tong, G.B. and Zhang, H.J. (2006), "Experimental research on RC eccentric compression column strengthened with the combination of CFRP and angle steel", *J. Build. Struct.*, **27**(1), 106-111.
Lu, Y.Y., Zhang, H. and Zhang, H.J. (2007), "Experimental study on the shear behavior of reinforced concrete columns strengthened with bonded steel angles combining with carbon fiber reinforced polymer sheets", *China Civ. Eng. J.*, **40**(10), 1-7.
Maaddawy, T.E., Sayed, M.E. and Abdel-Magid, B. (2010), "The effects of cross-sectional shape and loading condition on performance of reinforced concrete members confined with Carbon Fiber-Reinforced Polymers", *Mater. Design*, **31**(5), 2330-2341.
Montuori, R. and Piluso, V. (2009), "Reinforced concrete columns strengthened with angles and battens subjected to eccentric load", *Eng. Struct.*, **31**(2), 539-550.

BU